

# Powertrain fault diagnosis of manufacturing processes by means of servo drives

Johann Kolb  
Institute of Electrical Machines (IEM)  
RWTH Aachen University  
Aachen, Germany  
johann.kolb@iem.rwth-aachen.de

Andreas Thul  
Institute of Electrical Machines (IEM)  
RWTH Aachen University  
Aachen, Germany  
andreas.thul@iem.rwth-aachen.de

Kay Hameyer  
Institute of Electrical Machines (IEM)  
RWTH Aachen University  
Aachen, Germany  
kay.hameyer@iem.rwth-aachen.de

**Abstract** — During cyclical manufacturing processes, powertrain and process faults such as friction, distributed damage and material fatigue can occur. The early detection of faults through condition monitoring allows to minimize production losses and cost. Here, a condition monitoring approach is presented, which detects irregular deviations from the wished operation via the servo drive and does classify them. The approach distinguishes into signal analysis, characterization and classification. The analysis is summarized by characterization in representative values. The subsequent classification compares the characterization values of the measurement cycle with a reference cycle and classifies these into different classes, e.g. by pattern recognition. Various fault characteristics were simulated on a HiL test bench and the presented procedure was applied to the measurement variables rotational speed and torque-generating current of the servo drive. It can be stated that a predominant share of test cases is appropriately classified.

**Keywords**— condition monitoring, fault diagnosis, servo drive, manufacturing faults, predictive maintenance, pattern recognition.

## I. INTRODUCTION

A common application of servo drives is the utilization in production lines such as for packaging or filling operation. The machines are operated in process cycles with a high cycle frequency. Due to the high number of involved components, faults can occur in the electric drive or in the manufacturing process, which can negatively influence the product quality. As a result, unplanned downtime of production facilities occur. In order to minimize the failure rate and thus increase the efficiency of the system, an online diagnosis of the machine is suitable. By early detection of deviations in the drive system and in the production process, downtimes can be minimized and the predictability of maintenance can be improved. Condition monitoring is already part of the monitoring of mechatronic systems. Previous work was about the creation of comparative data, error indexing and self-learning process models. For this purpose, model-based process models are described which calculate dynamic process envelope data and can generate tolerances for the error comparison from the database [1]. Furthermore, the implementation for real-time computation is a research subject [2], [3]. Another focus is the self-diagnosis of the servo drives. The effects of magnetization errors, bearing and gear damage and the effect of eccentricities on the stator current are examined in [4], [5], [6].

In this paper, a condition monitoring approach is presented, which detects irregular deviations in powertrain and manufacturing processes with the existing sensors of the

servo drive system. Several condition monitoring procedures studied fault detection based on measurement signals. The analysis is performed time-based with operating limits or frequency-based with determined fault frequencies. Model-based approaches are a focus in nowadays research activities. The procedures are mostly developed for specific use cases and are therefore often not applicable as generic condition monitoring scheme for production machines. Faults are often detected after reaching an operational limit only. However, instead they should be identified in an early state of fault.

For the general condition monitoring all of the mentioned types of analysis should be considered. Therefore, this generic, non-static approaches use multiple analysis methods and pattern recognition to classify the signal deviations into classes. For this purpose certain analysis are combined to detect fault characteristics such as time-based, frequency-based and model-based methods. In section II, signal types of fault characteristics are described. Subsequently, in section III the procedure is discussed with different methods, which can analyze several signal types. The functionality of the procedure is validated on a hardware-in-the-loop test bench (section IV). Finally, concluding remarks are drawn in section V.

## II. CLASSIFICATION AND IDENTIFICATION OF SIGNAL DEVIATIONS

Powertrain and process faults affect the servo drive system in various forms. This can be e.g. friction, single and distributed damage, material fatigue and process faults. Possible faults can be divided into different signal types, which in turn can be analyzed by different methods. As a result, irregular deviations are detected by analyzing the following signal types: constant, periodic-harmonic

TABLE I. POSSIBLE SIGNAL DEVIATIONS IN THE TORQUE-FORMING CURRENT/ CALCULATED TORQUE.

Signal deviation	Signal type	Example	
		Categorization	Fault
Constant deviation	Constant	Friction	Faulty bearing
	Harmonic	Eccentricity	Faulty shaft alignment
Harmonics	Periodic	Individual fault	Bearing damage,
			gear tooth damage
Noise	Stochastic	Distributed faults	Wear of bearings and gears
			Play, process fault
Pulse	Aperiodic	Impact	

TABLE II. POSSIBLE SIGNAL DEVIATIONS IN THE ROTATIONAL SPEED.

Signal deviation	Signal type	Categorization	Example Fault
Constant deviation	Constant	Slip	Faulty belt drive
Harmonics	Periodic	Control	Faulty parameterization
Noise	Stochastic	Distributed faults	Wear of bearings and gears
Pulse	Aperiodic	Impact	Play, process fault

(sinusoidal), periodic-non-harmonic (impulse-shaped), stochastic and aperiodic deviations. The relevant measurement variables in the servo drive system are the torque-generating current or the calculated torque and the rotational speed. It should be noted that an irregularity can simultaneously affect different types of signals in different quantities. Tab. I shows the fault characteristics for the torque/torque-generating current, Tab. II for the rotational speed. For example, a worn belt drive could increase natural vibrations and thus trigger periodic harmonics in the torque.

### III. GENERIC, NON-STATIC PROCEDURE FOR CONDITION MONITORING

The proposed procedure is determined to record the condition of the system and to detect and classify any abnormalities or deviations. As a prerequisite for the approach, the servo drive system has to operate in a repetitive process cycle so that measurement cycles can be compared to a reference. This reference cycle represents the system in its state without damage or process faults. This cycle is used to detect and classify deviations based on the differences between the measurement cycle that represents the current state of the system. The aim of the procedure is to analyze the measurements, to characterize them afterwards and to classify the difference to the reference based on the three categories “good”, “warning”, and “error”. Fig. 1 illustrates this procedure. In the first step, measured data are recorded and preprocessed with the machine control. This is, for example, the calculated torque from the current sensors and the calculation of the rotational speed from the encoder signal. The processed data form the basis for further analysis.

The analysis methods are distinguished in the categories time-based, frequency-based and model-based. As depicted in section II, different analysis approaches must be used to analyze different types of signals. While the time-based analysis summarizes the measurements in characteristic values, additional data are generated by the frequency and model based analysis, e.g. frequency- and time-dependent data. These are not directly appropriate for a classification and must be characterized by representative values. The resulting characteristic values are suitable for classification by comparing them to the reference cycle characteristics. The analysis is done for one production cycle with the sample variable  $x$ , sample count  $n$  and cycle time  $t$ .

#### A. Time-based analysis

For the time-based analysis, different functions to describe distributions can be used. The mean value  $\mu(x)$  describes the average of the time-based signal. This has the advantage that systematic deviations are clearly recognized, but deviations can cancel each other out. However, the mean value is not sufficient for the detection of noise and vibrations [7].

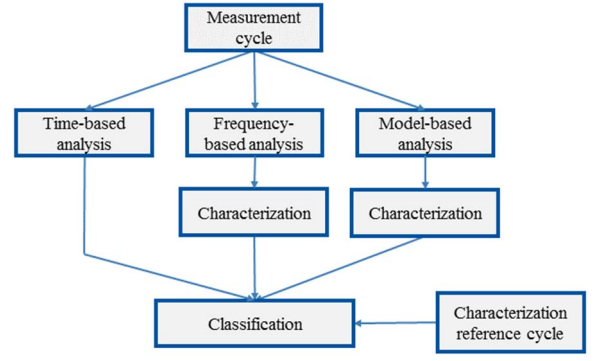


Fig. 1. Generic, non-static procedure for Condition Monitoring.

$$\mu(x) = \bar{x} = \frac{1}{n} \sum_{i=1}^n x_i \quad (1)$$

The standard deviation  $\sigma(x)$  is a measure of the deviations from the mean  $\mu(x)$ . Thereby, the width of the scattering can be easily recognized; however, no specific statement can be made about the extent of scattering [7].

$$\sigma(x) = \sqrt{\frac{1}{n-1} \sum_{i=1}^n (x_i - \bar{x})^2} \quad (2)$$

Further functions, such as skewness  $s_{sk}$ , kurtosis  $s_{ku}$ , crest factor and form factor can further characterize the distribution [7]. Yet the functions cannot always provide a meaningful result over the time course of the signal, e.g. aperiodic deviations are difficult to detect [8], [9], [10].

$$s_{sk}(x) = \frac{\mu[(x_i - \bar{x})^3]}{\sigma^3} \quad (3)$$

$$s_{ku}(x) = \frac{\mu[(x_i - \bar{x})^4]}{\sigma^4} \quad (4)$$

Other functions for the time-based analysis include the calculation of the root mean square (RMS), covariance, principal component analysis (PCA) and an improved PCA procedure for condition monitoring (AVPCA) [11],[12].

#### B. Frequency-based analysis

Frequency-based methods calculate the frequency of the measured signal and can primarily detect periodic deviations. The output used here for further analysis is the power spectral density (PSD) of the signal. The Fast Fourier Transformation (FFT) calculates the frequency spectrum from a time signal. Since the time information is not considered, only stationary processes should be used for an analysis. Because of the harmonic approach functions, periodic-harmonic signals are well suited for the detection [13]. The PSD  $S_F$  is calculated as the squared magnitude of the FFT function  $X_F(f)$ .

$$S_F(f) = |X_F(f)|^2 \quad (5)$$

One method that obtains the time information is the Short-Time Fourier Transform (STFT). The frequency spectrum  $S_{ST}$  is the Fourier transformation calculated for short time periods  $t$  such that frequency changes in the time signal become visible.

$$S_{ST}(f, t) = |X_{ST}(f, t)|^2 \quad (6)$$

The Continuous Wavelet Transform (CWT)  $S_W$  works similarly to the STFT. It is based on a non-harmonic approach function (wavelet). This makes the method well suited for the analysis of non-harmonic signals and can detect points of discontinuity better than the STFT [7].

$$S_C(f, t) = |X_W(f, t)|^2 \quad (7)$$

Other frequency-based methods, are for example the discrete Gabor transformation, which is derived from the STFT. In the same way as the STFT, this method is useful for periodic harmonic signals [17]. A different method is the envelope analysis (Hilbert transformation), which calculates the envelope of the time signal (demodulation) [6]. The envelope can be evaluated, e.g. with the CWT. Low-frequency modulation signals become more visible. On the other hand, higher-frequency signal components are neglected [6].

### C. Model-based analysis

The model-based analysis uses a model of the servo drive system. The corresponding method calculates the prediction of the time signal as the reference. From the difference to the reference cycle conclusions about possible irregular deviations can be drawn.

The Kalman filter performs a prediction of the state variables based on a state space model and measurement uncertainties. For this approach it is required to know the basic physical relations. Here, the resulting estimation error can be used to analyze deviations and to detect the faults. An advantage of the method with a known system structure is the precise prediction of the desired state of the signal. From this, the deviations from the nominal state of the system can be calculated and analyzed. However, it is possible that high-frequency error components cannot be detected [15].

Another method is the linear prediction. This approach performs the signal prediction on the basis of a linear system of equations. The coefficients must be determined by the reference cycle. Here, the error detection employs the analysis of the estimation error. One advantage is the ease of processing, but higher prediction errors can occur with large signal fluctuations [16], [17].

### D. Further analysis methods

Since Condition Monitoring essentially involves the recognition of patterns in the time signals, a view to the field of speech processing is interesting and appropriate. One approach in speech recognition is feature sequencing. An attempt is made to extract a sequence of features from a signal. For Condition Monitoring, one could assume that a characteristic is a possible failure characteristic. With knowledge of the characteristics, this would enable targeted detection of irregular deviations in the signal. To describe characteristics, statistical methods are also used here. A generalized approach here is the Hidden-Markov model, which is a statistical description of observation sequences [17]. Furthermore, methods of machine learning (e.g., "data mining" and "knowledge discovery in databases") may be used, which classify the measurement data based on trained data.

### E. Characterization

The data of the frequency- and model-based analysis methods in part B and C are not directly suitable for classification and must be combined to characteristic values. On the one hand, this considerably reduces the amount of variables for further processing, on the other hand, classification models can be trained in a more targeted manner. In a first step, the characterization should be subdivided into different set point sections of the process cycle, e.g. areas of constant speeds and ramps to avoid information loss in different operating states, e.g. frequency

interferences. Furthermore, a subdivision by frequency band is appropriate. A division of the frequency band as a function of the fundamental mechanical frequency  $f_N$  can be defined as

$$f_{B,k} = k \cdot f_N, \quad (8)$$

which is valid for the rotating speed. For the torque-generating current and the calculated torque

$$f_{B,k} = (p + k)f_N \quad (9)$$

has to be used, where  $p$  is the number of pole pairs. The maximum relevant side band structures which should be included for further analysis, can be estimated with a maximum of  $k_{max} \approx 20$  [18].

For the combination of time- and frequency-dependent data sets stochastic methods are suitable, as described for the time-based analysis (part A). Thus, for example the mean PSD of a frequency band  $f_{B,k}$  as a characteristic value is calculated with (1) as

$$\mu_S(f_{B,k}, t) = \frac{1}{n_f} \sum_{f=f_{B,k}}^{f_{B,k+1}} S(f, t) \quad (10)$$

and the standard deviation according to (2) as

$$\sigma_S(f_{B,k}, t) = \sqrt{\frac{1}{n_f - 1} \sum_{f=f_{B,k}}^{f_{B,k+1}} (S(f, t) - \bar{S}(f_{B,k}, t))^2}, \quad (11)$$

where  $n_f$  is the count of frequency bins between  $f_{B,k}$  and  $f_{B,k+1}$ .

The calculation of the characterization values  $CV$  for the set point sections are equivalent to the calculation of the stochastic values for the frequency band sections. Thus, the mean is defined according to (10) as

$$CV_\mu(k, l) = \frac{1}{n_t} \sum_{t=n_t(l)}^{n_t(l+1)} \mu_S(f_{B,k}, t) \quad (12)$$

and the standard deviation in relation to (11) as

$$CV_\sigma(k, l) = \frac{1}{n_t} \sum_{t=l}^{l+1} \sigma_S(f_{B,k}, t), \quad (13)$$

where  $n_t$  is the number of time samples between the set point sections  $l$  and  $l + 1$ .

The calculation of the characterization values for other stochastic functions is equal to (12) and (13).

### F. Classification

The classification represents the last step of the approach. It is adapted to classify the irregularities into "good", "warning" and "error". For this purpose, in the first step, the differences between characterization results of measurement and reference cycle are calculated.

$$\Delta CV = CV_{Meas} - CV_{Ref} \quad (14)$$

The classification of the difference in the characterization values can be done manually or automatically. For manual classification, warning and fault limits are taken from previous measurements and determined based on empirical values. It should be noted, that not every disproportionate change in the difference values corresponds to a fault characteristic. These

may be e.g. natural frequencies of the system, which cause an increase without an irregular deviation.

Another possibility for a more complex classification method is an automatic classification algorithm. This requires training data sets that contain as many states of the system as possible. Training data contains the reference state of the servo drive system as well as various types of fault conditions that cause irregular deviations in the different measurement variables.

The training matrix  $\mathbf{T}$  subsequently is built with the different states of the system  $c$ , signal types  $n$ , stochastic methods  $s$ , frequency bands up to  $k_{max}$  and set point sections up to  $l_{max}$ . In machine learning the column entries are considered as categories.

$$\mathbf{T} = \begin{bmatrix} \Delta CV_{1,1,1}(1,1) & \cdots & \Delta CV_{1,s,n}(k_{max}, l_{max}) \\ \vdots & \ddots & \vdots \\ \Delta CV_{c,1,1}(1,1) & \cdots & \Delta CV_{c,s,n}(k_{max}, l_{max}) \end{bmatrix} \quad (15)$$

The order of the different category values in a row is trivial, but has to be consistent for training and classification.

A possible classification model is the Naïve Bayes classifier. To each training data set, which is equivalent to system state  $c$ , a class is assigned. Subsequently, the parameters of the model are calculated such that an optimal classification of the data set is given. Consequently, newly recorded data sets are automatically assigned to a class in the best possible way.

#### IV. EXAMINATION ON THE TEST BENCH

The examination on the test bench validates the functionality of the approach described in section III. Since no machines with different types of fault characteristics were available for the examination, a hardware-in-the-loop (HiL) test setup is used for further examinations. The test bench consists of a speed-controlled device under test (DUT) and a torque-controlled load machine (Fig. 2). The DUT represents the servo drive to be evaluated, from which the measurement data are recorded. The load machine emulates a typical powertrain with corresponding faults characteristics. The machines are coupled with a single-stage belt transmission. The load machine also has an auxiliary gearbox with  $i = 8$ .

##### A. Emulation of the crankshaft model

The exemplary, industry-oriented powertrain model consists of a crankshaft that moves a mass (Fig. 3). Non-uniform translating gears are often used in the process industry

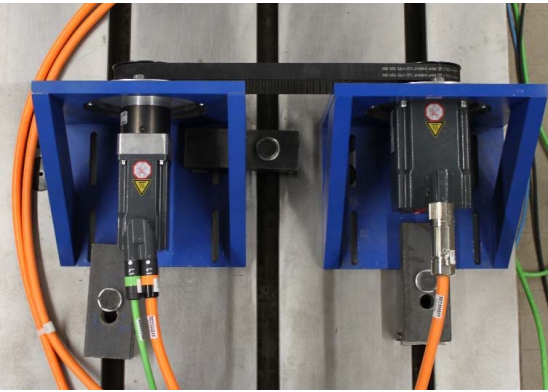


Fig. 2. Test bench structure (device under test right, load machine left).

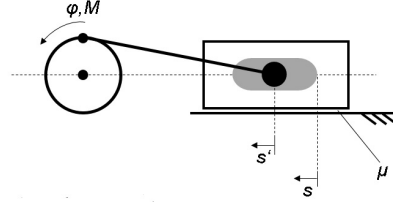


Fig. 3. Crankshaft model.

and represent a real use case. The model considers play  $\Delta s$ , friction  $\mu$  and eccentricity  $A_{ecc}$ .

The linear movement of the crankshaft is described as

$$s' = r \left( 1 + \frac{1}{\lambda} - \cos \varphi - \sqrt{\frac{1}{\lambda^2} - \sin^2 \varphi} \right), \quad (16)$$

where  $\lambda$  is the ratio between the crankshaft and the connection rod,  $r$  the length of the crank and  $\varphi$  the angle of the crankshaft. The play between the crankshaft and the mass with movement  $s$  is defined as

$$\Delta s = s - s'. \quad (17)$$

The contact force in the bearing is defined as a nonlinear spring-damper-element. This describes the material behavior of an inelastic collision of the mass and connection rod as well as the movement of play.

$$F_B(\Delta s, \Delta \dot{s}) = \text{sgn}(\Delta \dot{s}) \cdot (e^{c_B \Delta s} - 1) \cdot \Delta s^{a_B} + d_B \cdot \Delta \dot{s} \quad (18)$$

The constants  $c_B$  and  $a_B$  are defined as the nonlinear spring characteristic and  $d_B$  the damping constant.

The friction between ground and mass is divided in static  $\mu_S$  and dynamic  $\mu_D$  friction depending on the play velocity.

$$F_F(\Delta \dot{s}) = \begin{cases} \text{sgn}(\Delta \dot{s}) \cdot m \cdot g \cdot \mu_D + d_F \cdot \Delta \dot{s}, & \Delta \dot{s} <> 0 \\ m \cdot g \cdot \mu_S + d_F \cdot \Delta \dot{s}, & \Delta \dot{s} = 0 \end{cases} \quad (19)$$

The movement of the mass is a second order differential equation with the mass  $m$ .

$$\ddot{s} = -\frac{1}{m} (F_B(\Delta s, \Delta \dot{s}) + F_F(\Delta \dot{s})) \quad (20)$$

The operating torque  $M_{cr}$  on the shaft of the connection rod is therefore calculated with

$$M_{cr}(\varphi) = r \cdot \sin \varphi \cdot F_F(\Delta s, \Delta \dot{s}). \quad (21)$$

The dependence between angle and time is here considered as linear:

$$\varphi = \omega \cdot t \quad (22)$$

The eccentricity is appended to the torque with the amplitude  $A_{ecc}$  and frequency  $f_{ecc}$ .

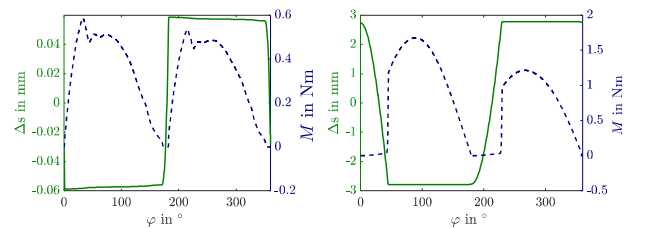


Fig. 4. Calculated set point values as reference state (left) and maximum failure state (right).

$$M(\varphi) = M_{cr}(\varphi) \cdot \left[ 1 + A_{ecc} \cdot \sin\left(2\pi \cdot f_{ecc} \cdot \frac{\varphi}{\omega}\right) \right] \quad (23)$$

The differential equation is solved until the initial numerical oscillation has subsided, so that the set points for the load machine is derived from one revolution of the rotor. The play  $\Delta s$  is varied between 0.1 mm and 5.4 mm, the friction coefficient  $\mu$  from 0.1 to 0.4 and the eccentricity from 0% to 10% of the load. All combinations of the different types of faults results in 112 measurements. There are 12 additional test cases which will not be used for the classification training. Fig. 4 shows the calculated set point values for the reference and the maximum fault state. In the reference cycle there is a minimum of play and modest torque, while the maximum of fault cycle has a significant higher play and torque, caused by the friction and eccentricity.

### B. Data analysis

The data of the DUT are measured for three seconds and evaluated with the time-based ( $\mu$ ,  $\sigma$ ,  $s_{sk}$ ,  $s_{ku}$ ) and frequency-based analysis (FFT, STFT and CWT). These are performed for each torque and speed measurement over the measurement cycle.

Fig. 5 shows the FFT of the torque for reference and maximum fault state. In the region of low frequencies there are some Eigenfrequencies visible and in the reference state a rise around 100Hz is roughly noticeable. In the time-dependent STFT (Fig. 6) and CWT (Fig. 7) the higher power densities in low frequency regions as well as the rise around 100 Hz are apparent. In the different fault states no characteristic frequencies are detectable that can be related to the type and intensity of the fault.

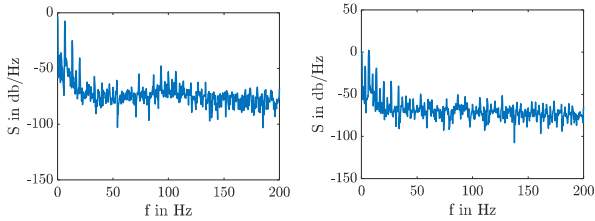


Fig. 5. Calculated FFT of the torque as reference state (left) and maximum fault state (right).

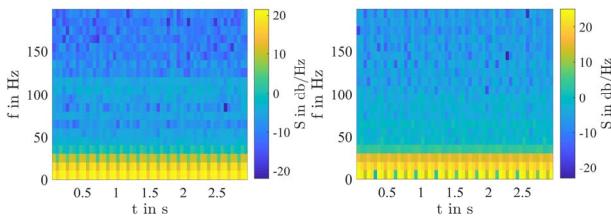


Fig. 6. Calculated STFT of the torque as reference state (left) and maximum fault state (right).

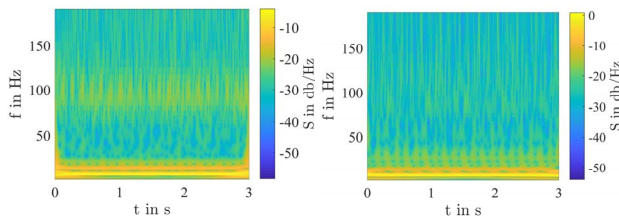


Fig. 7. Calculated CWT of the torque as reference state (left) and maximum fault state (right).

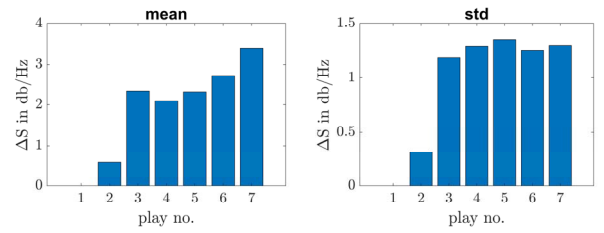


Fig. 8.  $\Delta CV_{\mu}$  (left) and  $\Delta CV_{\sigma}$  (right) for the FFT for different intensities of play.

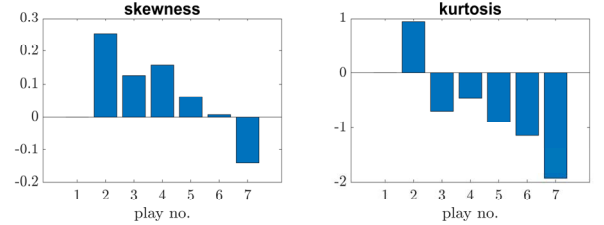


Fig. 9.  $\Delta CV_{s_{sk}}$  (left) and  $\Delta CV_{s_{ku}}$  (right) for the FFT for different intensities of play.

### C. Classification

The characterization for the STFT and CWT are also performed with the time-based methods  $\mu$ ,  $\sigma$ ,  $s_{sk}$  and  $s_{ku}$ . The resulting differences of characterization values  $\Delta CV_{\mu}$ ,  $\Delta CV_{\sigma}$ ,  $\Delta CV_{s_{sk}}$  and  $\Delta CV_{s_{ku}}$  serve as input for the training matrix for classification. Fig. 8 and fig. 9 show the differences of the characterization values for mean  $\Delta CV_{\mu}$ , standard deviation  $\Delta CV_{\sigma}$ , skewness  $\Delta CV_{s_{sk}}$  and kurtosis  $\Delta CV_{s_{ku}}$  of the FFT for different intensities of play. A rise in the mean as well as in the standard deviation are clearly visible. The skewness and also the kurtosis are decreasing with an increasing intensity of play.

The training matrix is built as described in section III.F with (15). With the two measurement variables torque and speed, four types of stochastic analysis for time and frequency-based methods and three types of frequency analysis as well as 112 system states the training matrix has a size of  $112 \times 32$ .

The Naïve Bayes classifier is used for training and classification. In the first step, the optimum parameters of the classifier are determined from the training matrix. Then, for the twelve test cases the differences of the characterization values are calculated. Subsequently, the classification input vector is built in the same manner as building the training matrix for one system state (15).

The test cases are then classified and give a correct result in nine out of twelve cases. In Fig. 10 the results of the estimated classification of the Naïve Bayes classification are plotted against the correct classification. In two falsely

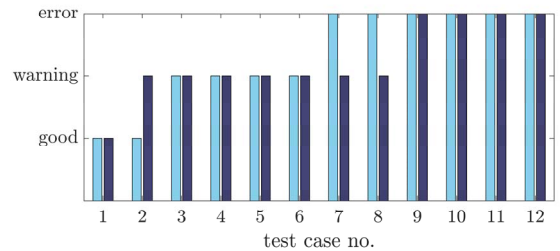


Fig. 10. Classification results of the twelve test cases; predicted classification on the left bars and correct results on the left bars.

classified cases (no. 7 and 8), the classifier specified the data as an error instead of a warning. Because the two model parameters are classified as warnings and superimposed in the measurement, the estimated classification could be also seen as a correct result. In case no. 2 the algorithm classifies the data as normal rather than as a warning, because of minimum fault parameter variation from the reference state.

## V. CONCLUSIONS

Powertrain and process faults can be caused e.g. by friction, single and distributed damage, material fatigue, and process faults. The faults cause different types of signal deviations in the measurement variables of the servo drive, such as in the torque-generating current and rotational speed.

The presented condition monitoring approach considers various methods. The developed procedure analyzes the different signal deviations, summarizes the deviations and compares them with the recorded data of a reference cycle. For this purpose, the procedure is split into analysis, characterization and classification. The analysis distinguishes into time-based, frequency-based and model-based methods and examines the different measurement variables with regard to the signal deviations. The subsequent characterization utilizes functions to summarize time and frequency dependent data. The classification compares the characterization values of the measurement cycle with those of the reference cycle and classifies them to the classes "good", "warning" and "error" manually or automatically. For manual classification, limits are set for the difference values based on calculation bases or empirical values. The automatic classification is based on a classification model from the pattern recognition scope. The classifier is trained with the differences of the characterization values from recorded measurement cycles according to the classes in such a way that new measurement cycles are automatically classified into the classes.

The procedure was examined on a test bench. The test bench consists of a speed-controlled device under test (DUT) and a load machine. With the load machine, a crankshaft is emulated and play, friction and eccentricity are considered. In total 112 measurements are done for training and twelve for testing purposes. Rotational speed and torque-generating current of the DUT are analyzed with the presented procedure. As a result no characteristic frequencies are detectable that can be related to the type and intensity of the different fault states. The classification is done with the Naïve Bayes classifier, which is trained with combinations of fault characteristics from measurement. To validate the procedure, the test cases were analyzed with fault characteristics unknown to the classifier. The fault characteristics were classified correctly in nine out of twelve cases. Thus, a predominantly correct classification is given. In future, the procedure should be examined on production machines to investigate the influence of individual analysis method to the classification and to improve the pattern recognition.

## VI. ACKNOWLEDGMENT

The authors like to thank the German Research Association for Power Transmission Engineering (FVA) and Food Processing and Packaging Machinery Association of the

German Engineering Federation VDMA, as well as Mr. Fertig (Fertig Motors GmbH) and Mr. Philipp (Robert Bosch Packaging Technology B.V) for supporting the work.

## REFERENCES

- [1] S. Windmann and O. Niggemann, „Efficient Fault Detection for Industrial Automation Processes with Observable Process Variables”, In Proc. 2015 IEEE 13th International Conference on Industrial Informatics (INDIN), pp. 121-126, 2015.
- [2] S. Windmann and O. Niggemann: „A GPU-based method for robust and efficient fault detection in industrial automation processes”, In Proc. IEEE 14th International Conference on Industrial Informatics (INDIN), pp. 442-445, 2016.
- [3] H. Fleischmann, J. Kohl and J. Franke, „A Modular Web Framework for Socio-CPS-Based Condition Monitoring”, In Proc. IEEE World Conference on Factory Communication Systems (WFCS), pp.1-8, 2016.
- [4] T. Herold, „Simulation des elektrischen Antriebsstrangs als Hilfsmittel für die Synthese und Überprüfung von Algorithmen im Kontext der antriebsbasierten Diagnose“, Dissertation, RWTH Aachen, 2016.
- [5] I. Coenen, „Beitrag zur Analyse elektrischer Antriebssysteme mit toleranzbehafteten Komponenten: Vom elektromagnetischen Entwurf bis zur End-of-Line Prüfung“, Dissertation, RWTH Aachen, 2015.
- [6] C. Piantsof Mbo’o, C. Lessmeier, D. Zimmer and K. Hameyer, „Frequenzselektiver Schadensindikator für die Diagnose von Wälzlagerschäden im elektrischen Antriebsstrang”, antriebstechnik, vol. 5/2017, Forschungsvereinigung Antriebstechnik, 2017.
- [7] R. Waldi, Statistische Datenanalyse. Berlin Heidelberg: Springer Spektrum, 2015.
- [8] D. Zimmer, C. Lessmaier, C. Piantsof Mbo’o, I. Coenen and K. Haymeyer, „Untersuchung von Bauteilschäden elektrischer Antriebsstränge im Belastungsprüfstand mittels Statorstromanalyse“, In Proc. Aachener Kolloquium für Instandhaltung, Diagnose und Anlagenüberwachung, pp. 509-521, 2012.
- [9] C. Piantsof Mbo’o and K. Hameyer, „Bearing damage diagnosis by means of the linear discriminant analysis of stator current feature”, In Proc. 2015 IEEE 10th International Symposium on Diagnostics for Electrical Machines, Power Electronics and Drives (SDEMPED), pp. 296-302, 2015.
- [10] C. Piantsof Mbo’o and K. Hameyer, „Fault Diagnosis of Bearing Damage by Means of the Linear Discriminant Analysis of Stator Current Features From the Frequency Selection”, IEEE Transactions on Industry Applications, Vol. 52, pp. 3861-3867, 2016.
- [11] A. Handl, Multivariate Analysemethoden. Berlin Heidelberg: Springer-Verlag, 2010.
- [12] M. Hamadache, D. Lee and K. Velovolu, „Rotor Speed-Based Bearing Fault Diagnosis (RSB-BFD) Under Variable Speed and Constant Load”, IEEE Transactions on industrial Electronics, Vol. 62., pp. 6486-6494, 2015.
- [13] C. Piantsof Mbo’o, T. Herold and K. Hameyer, „Impact of the load in the detection of bearing faults by using the stator current in PMSM’s”, In Proc. 2014 International Conference on Electrical Machines (ICEM), pp. 1615-1621, 2014.
- [14] K. Kristian, G. Rigoll and B. Schuller, Statistische Informationstechnik. Berlin Heidelberg: Springer-Verlag, 2011.
- [15] R. Marchthaler and S. Dingler, Kalman-Filter. Berlin Heidelberg: Springer Vieweg, 2017.
- [16] R. Hoffmann and M. Wolff, Intelligente Signalverarbeitung 1. Berlin Heidelberg: Springer Vieweg, 2014.
- [17] B. Pfister und T. Kaufmann, Sprachverarbeitung. Berlin Heidelberg: Springer Vieweg, 2017.
- [18] T. Herold, C. Piantsof Mbo’o and K. Hameyer, „Evaluation of the use of an electrical drive as a sensor for the detection of bearing damage”, In Proc. Conference on Acoustics, AIA-DAGA 2013, pp. 1538-1540, 2013.